End-on cyanate or end-to-end thiocyanate bridged dinuclear copper(II) complexes with a tridentate Schiff base blocking ligand: Synthesis, structure and magnetic studies

Samim Khan,[a] Stephen Sproules,[b] Louise S. Natrajan,[c] Klaus Harms,[d] Shouvik Chattopadhyay[a,*]

[a] *Department of Chemistry, Inorganic Section, Jadavpur University, Kolkata – 700 032, India.*

[b]*WestCHEM, School of Chemistry, University of Glasgow, Glasgow G12 8QQ, United Kingdom.*

[c]*School of Chemistry, The University of Manchester, Oxford Road, Manchester M13 9PL, United Kingdom.*

[d]*Fachbereich Chemie, Philipps-Universität Marburg, Hans-Meerwein-Straße, D-35032 Marburg, Germany.*

Abstract: Two dinuclear copper(II) complexes, *[$Cu_2(L)_2(\mu_{1,1}$-$NCO)_2$]* (**1**) and *[$Cu_2(L)_2(\mu_{1,3}$-$NCS)_2$]·H_2O·DMF* (**2**) have been synthesized using a tridentate N_2O donor Schiff base ligand (HL) [1((2-(ethylamino)ethylimino)methyl)naphthalen-2-ol] and characterized by elemental analysis, spectral study and X-ray crystallography. Both complexes are centrosymmetric dimers in which square pyramidal copper(II) centres are connected by pseudo-halides; end-on cyanate in **1** and end-to-end (EE) thiocyanate in **2**. Variable temperature (2–300 K) magnetic susceptibility measurements indicate the presence of ferromagnetic exchange coupling between copper(II) centres in complex **1** (J = 0.97 cm^{-1}), and antiferromagnetic exchange coupling in **2** (J = - 0.6 cm^{-1}).

Keywords: Copper(II), Schiff base; Crystal structures, Magnetic properties

Introduction

Designed synthesis of di and polynuclear copper(II) complexes is an interesting area of research for their diverse structures and potential applications in magnetic materials.[1] Although different bridging ligands have been employed for their synthesis, use of pseudohalide as bridging ligand in preparing such complexes is a common practice, as pseudohalides with various bridging modes can lead to the formation of complexes with surprising difference in the structures and magnetic properties.[2] The most widely used pseudo-halide is azide,[3] and the chemistry of azide coordinated complexes have already been reviewed.[4] On the other hand, although works on cyanato and thiocyanato bridged complexes are relatively less, reports on the synthesis and characterization of such complexes could also be found in literature.[5] The structures of cyanate and thiocyanate are very similar with both having linearly exposed N···C···X (X=O in cyanate and X=S in thiocyanate) skeleton. Both these ligands may be used as terminal ligands[6] and may be used as bridging ligands.[7] They may show end-on (EO) and/or end-to-end (EE) binding modes when act as bridging ligands.[8]

Focusing to copper(II), both type of bridges can be either symmetrical or unsymmetrical due to active Jahn–Teller effects on the metal centre which make the structures even more versatile.[9] The magnetic exchange via the pseudo-halide bridge can be ferro- or antiferromagnetic. When pseudo-halide ligand bridges two copper(II) centres in an end-on, basal–basal manner, ferromagnetic exchange coupling is observed only when the value of Cu–N–Cu angle is less than 109°, whereas antiferromagnetic exchange coupling is observed when the value of Cu–N–Cu angle is 109°.[10] On the other hand, any meaningful overlap between magnetic orbitals is absent for end-on basal–apical bridges leading to very small magnetic couplings.[11] Same is the case for the end-to-end pseudo-halide bridged complexes due to

relatively longer distance between the copper(II) centres.[12] In the present work, a tridentate Schiff base, 1((2-(ethylamino)ethylimino)methyl)naphthalen-2-ol, (HL) has been used to prepare two copper(II) complexes in presence of cyanate and thiocynate coligands. It has been observed that cyanate forms EO bridges and thiocyanate forms EE bridges to form two centrosymmetric dinuclear complexes, *$[Cu_2(L)_2(\mu_{1,1}\text{-}NCO)_2]$* (**1**) and *$[Cu_2(L)_2(\mu_{1,3}\text{-}NCS)_2]\cdot H_2O\cdot DMF$* (**2**) respectively. Variable temperature magnetic susceptibility was measured. EE thiocyanate transmits antiferromagnetic interactions, whereas EO cyanate transmits ferromagnetic interactions among copper(II) centres in **1** and **2** respectively.

Preparations

*Preparation of $[Cu_2(L)_2(\mu_{1,1}\text{-}NCO)_2]$ (**1**)*

The Schiff base ligand, HL, was prepared by the condensation of N-ethyl-1,2-diaminoethane (0.105 mL, 1 mmol, 0.837 g/mL) and 2-hydroxy-1-acetonaphthone (186 mg, 1 mmol) in methanol solution under reflux for ca. 1 h. The Schiff base ligand was not isolated. A methanol (10 mL) solution of copper(II) acetate monohydrate (200 mg, 1 mmol) was added into the methanol solution of the ligand followed by addition of methanol-water solution of sodium cyanate (65 mg, 1 mmol) with constant stirring. The stirring was continued for an additional ca. 2 h. Dark green single crystals, suitable for X-ray diffraction, were obtained after few days by slow evaporation of dark green acetonitrile solution of the compound in open atmosphere.

Yield: 267 mg [73.98%, based on copper (II)]; Anal. Calc. for $C_{34}H_{38}Cu_2N_6O_4$ (721.78): C, 56.58; H, 5.31; N, 11.64%. Found: C, 56.5; H, 5.4; N, 11.4%. ESI-MS (positive ion mode, acetonitrile) m/z: 678.24 $[\{Cu_2(L)_2(\mu_{1,1}\text{-}NCO)\}]^+$; 318 $[Cu(L)]^+$. FT-IR (KBr, cm^{-1}):3201 (ν_{NH}),

2215 (ν_{NCO}), 1615 ($\nu_{C=N}$); UV-Vis, λ_{max} (nm) [ε_{max}($Lmol^{-1}cm^{-1}$)] (acetonitrile): 310 ($1.3x10^4$), 387 (1.25×10^4), 595 ($2.61x10^2$).

*Preparation of $[Cu_2(L)_2(\mu_{1,3}\text{-}NCS)_2]\cdot DMF\cdot H_2O$ (**2**)*

It was prepared in a similar method as that of complex **1**, except that sodium thiocyanate (81 mg, 1 mmol) was used instead of sodium cyanate. Single crystals, suitable for X-ray diffraction, were obtained after few days on slow evaporation of the solution.

Yield: 318 mg [~67.9%, based on copper (II)]; Anal. Calc. for $C_{40}H_{56}Cu_2N_8O_6S_2$ (936.12): C, 51.32; H, 6.03; N, 11.97%. Found: C, 51.2; H, 6.1; N, 11.8%. ESI-MS (positive ion mode, acetonitrile) m/z: 696.07 [$\{Cu_2(L)_2(\mu_{1,3}\text{-}NCS)\}]^+$; 318 $[Cu(L)]^+$. FT-IR (KBr, cm^{-1}): 3227 (ν_{NH}), 2101 (ν_{NCS}), 1601 ($\nu_{C=N}$); UV-Vis, λ_{max} (nm) [ε_{max}($Lmol^{-1}cm^{-1}$)] (acetonitrile): 312 (1.45×10^4), 388 (1.21×10^4), 594 ($2.25x10^2$).

Result and discussion

Synthesis

The tridentate N_2O donor Schiff base ligand (HL) was produced by the condensation of N-ethyl-1,2-diaminoethane and 2-hydroxy-1-acetonaphthone following the literature method.[1a] The monocondensed Schiff base ligand, HL, on reaction with copper(II) acetate monohydrate and different pseudo-halides gave copper(II) complexes, $[Cu_2(L)_2(\mu_{1,1}\text{-}NCO)_2]$ (**1**) and $[Cu_2(L)_2(\mu_{1,3}\text{-}NCS)_2]\cdot(DMF)\cdot H_2O$ (**2**) (Scheme 1).

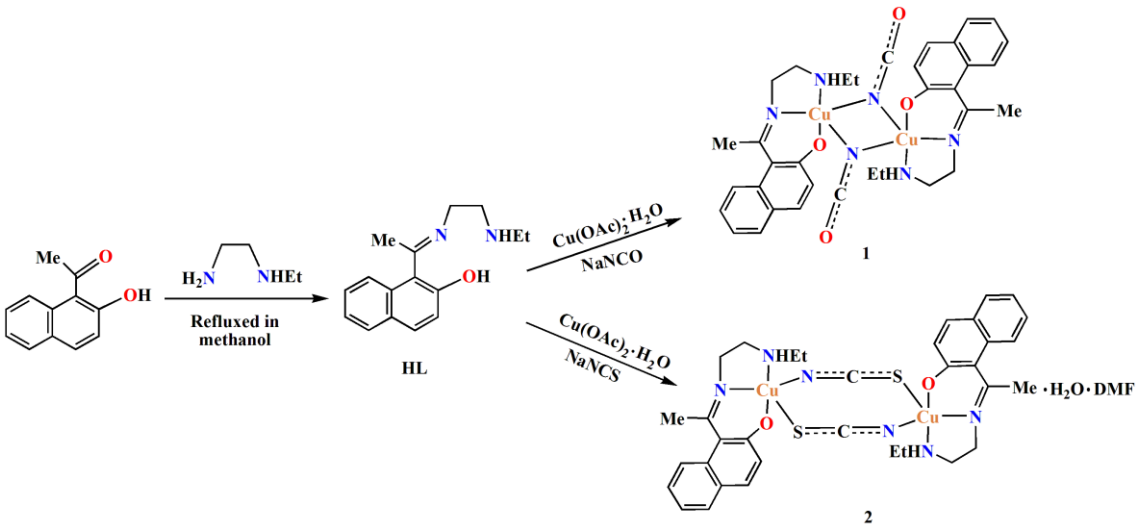

Scheme 1: Synthetic route to complexes

The reaction with cyanate and thiocyanate produced double end-on and end-to-end bridged copper(II) dimers, respectively. The structures of both complexes have been determined by single crystal X-ray diffraction analysis. The crystallographic and refinement data of both complexes are displayed in Table 1.

Table 1: Crystal data and refinement details of complexes **1** and **2**.

Complex	**1**	**2**
Formula	$C_{34}H_{38}Cu_2N_6O_4$	$C_{40}H_{56}Cu_2N_8O_6S_2$
Formula weight	721.78	936.12
Temperature(K)	100	100
Crystal system	Monoclinic	Monoclinic
Space group	$P2_1/c$	$P2_1/n$
a(Å)	11.4708(6)	15.5100(4)
b(Å)	14.4673(7)	7.1497(3)
c(Å)	9.4198(5)	19.7873(5)
β(°)	98.641(2)	101.121(2)

Z	2	2
d_{calc}(g cm^{-3})	1.551	1.444
μ(mm^{-1})	1.426	1.140
F(000)	748	980
Total reflections	31312	23622
Unique reflections	3554	4551
Observed data [I > 2σ(I)]	3310	3977
R(int)	0.023	0.023
R1, wR2 (all data)	0.0231, 0.0562	0.0281, 0.0748
R1, wR2 [I > 2σ(I)]	0.0207, 0.0550	0.0243, 0.0738

The difference in structures of both complexes may be related with the size of pseudo-halide co-ligands. Small cyanate prefers to bind in end-on fashion. This end-on bridged dimer gets extra-stability due to intra-dinuclear hydrogen bonding interactions. On the other hand, the larger thiocyanate prefers to bind copper centres in end-to-end fashion. The bridging ability of thiocyanate also favours to connect copper centres in end-to-end fashion.

Description of structures

*Complexes $[Cu_2(L)_2(\mu_{1,1}\text{-}NCO)_2]$ (**1**)*

Single crystal X-ray crystallography reveals that complex **1** is a centrosymmetric dimer and crystallizes in the monoclinic space group $P2_1/c$. The asymmetric unit contains a copper(II) centre, which adopts a elongated (4+1) square pyramidal geometry, bonded to three donor atoms (N,N,O) of the deprotonated tridentate Schiff base (L^-) and end-on bridging cyanate ligand. The perspective view of complex **1** with selective atom numbering scheme is depicted in Fig. 1.

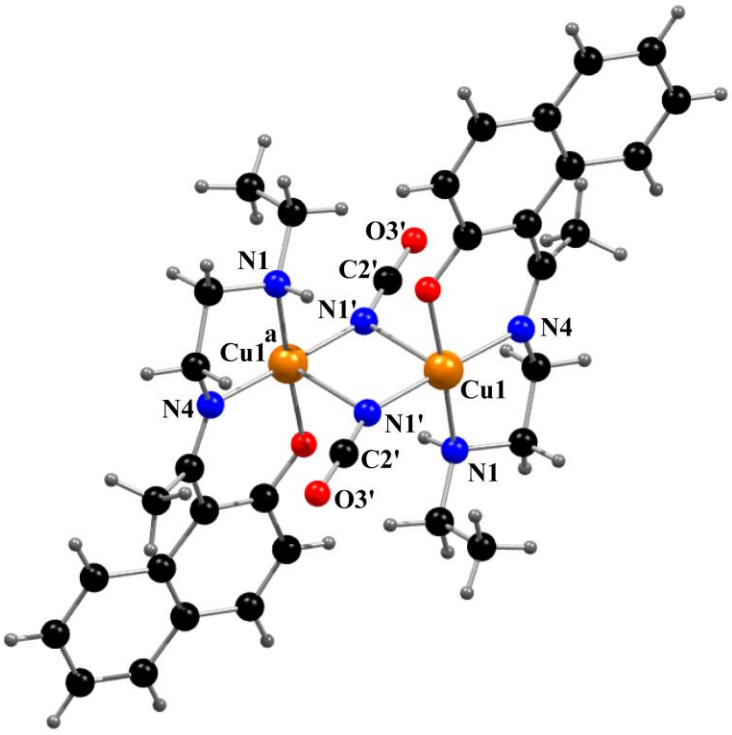

Fig. 1: Perspective view of complex **1** with selective atom numbering scheme. Hydrogen atoms have been omitted for clarity. Symmetry transformation: [a] = 1-x,1-y,1-z.

The Addison parameter[13] (trigonality index, $\tau = (\alpha-\beta)/60$, where α and β are the two largest L–M–L angles of the coordination sphere) is zero for a perfectly square pyramidal and is one for a perfectly trigonal bipyramidal complex. The Addison parameter value (τ) is 0.102 indicating the coordination sphere around copper(II) centre very close to ideal square-pyramidal geometry. As usual for square pyramidal structures, copper(II) centres are slightly pulled out of the mean square planes towards the apical donor atoms at distances of -0.0439(3) Å in **1**. The three donor atoms of the Schiff base occupy the equatorial plane while the anionic ligand in the dimer occupies an equatorial position in one copper coordination sphere and an axial position at a longer distance in the other. The Cu–N_{imine} distance (1.936(4) Å) is significantly shorter than the Cu–N_{amine} distance (2.028(5) Å), as was observed in similar complexes.[14] The five membered chelate ring Cu(1)–N(1)–C(2)–C(3)–N(4) assumes an intermediate conformation between half-

chair and envelope being twisted on C(2)-C(3) with puckering parameters[15] q(2) = 0.4152(14) Å and ϕ(2) = 265.81(15)°. Deviations of the coordinating atoms, N(1), N(4), O(7) and N(1'), from the least-square basal planes are 0.0765(12), -0.0579(12), 0.0811(10) and -0.0558(13) Å. The bridging pseudo-halide is quasi-linear with the N–C–O angle being 177.4(2)°. The intra-dimer Cu···Cu distance is 3.2354(4) Å. Selected bond lengths and angles are given in Tables 2 and 3, respectively.

Table 2: Selected bond lengths (Å) around the copper(II) in complexes **1** and **2**.

Complex	**1**	**2**
Cu(1)-O(7)	1.8963(10)	1.9316(11)
Cu(1)-N(1)	2.0374(11)	2.0457(14)
Cu(1)-N(1')	1.9375(12)	1.9635(14)
Cu(1)-N(4)	1.9504(12)	1.9572(13)
Cu(1)-N(1')[a]	2.7216(13)	1.958(3)
Cu(1)-S(3')[a]	-	2.7729(5)

The hydrogen atom, H(1), attached to the amine nitrogen atom, N(1), forms intra dimer hydrogen bond with the symmetry related ([a] = 1-x,1-y,1-z) phenoxo oxygen atom, O(7)[a], depicted in Fig. 2. The details of hydrogen bonding interactions are depicted in Table 4.

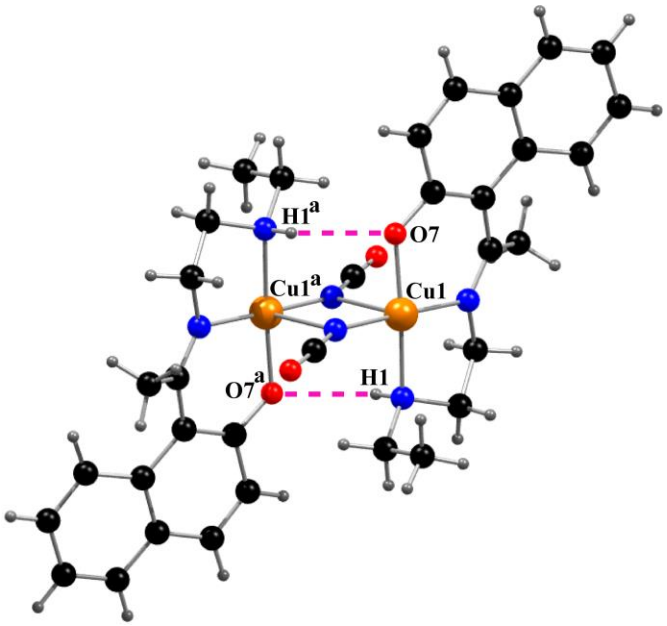

Fig. 2: Intra-dimeric hydrogen bonding interaction in complex **1**. Symmetry transformation, [a] = 1-x, 1-y, 1-z.

The phenyl rings [C(6)-C(7)-C(8)-C(9)-C(10)-C(15)] and [C(10)-C(11)-C(12)-C(13)-C(14)-C(15)], is involved in intermolecular π···π interactions with the symmetry related (2-x,1-y,2-z) phenyl ring C(10)-C(11)-C(12)-C(13)-C(14)-C(15), leading to the formation of 1D chain (Fig. 3). The geometric features of π···π and C–H···π interactions are gathered in Tables 5 and 6, respectively.

Table 3: Selected bond angles (^{0}) around copper(II) in complexes **1** and **2**.

Complex	**1**	**2**
O(7)-Cu(1)-N(1)	172.62(5)	164.89(5)
O(7)-Cu(1)-N(1')	88.76(5)	90.32(5)
O(7)-Cu(1)-N(4)	92.24(4)	90.39(5)
O(7)-Cu(1)-N(1')[a]	90.71(4)	98.69(4)
N(1)-Cu(1)-N(1')	93.05(5)	92.52(6)
N(1)-Cu(1)-N(4)	86.05(5)	85.53(5)

N(1)-Cu(1)-N(1')[a]	82.04(4)	-
N(1')-Cu(1)-N(4)	178.78(5)	174.96(6)
N(1')-Cu(1)-N(1')[a]	93.77(5)	-
N(1')[a]-Cu(1)-N(4)	86.92(4)	-
S(3')[a]-Cu(1)-N(1)	-	95.79(4)
S(3')[a]-Cu(1)-N(1')	-	95.89(4)
S(3')[a]-Cu(1)-N(4)	-	88.94(4)

Symmetry transformations: [a] =1-x,1-y,1-z, [b] =1-x, -y,1-z

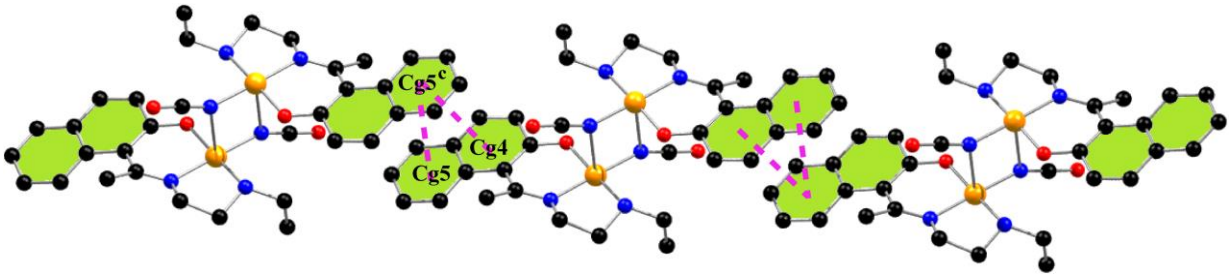

Fig. 3: Supramolecular one-dimensional chain of complex **1** formed via π···π interactions. Cg(4) and Cg(5) represent the centre of gravity of the rings [C(6)-C(7)-C(8)-C(9)-C(10)-C(15)] and [C(10)-C(11)-C(12)-C(13)-C(14)-C(15)] for complex **1**. Hydrogen atoms have been omitted for clarity.

Table 4: Geometric parameters for H-bonding interactions for complexes **1** and **2**.

Complex	**D–H···A**	**D–H (Å)**	**H···A (Å)**	**D···A (Å)**	**∠D–H···A (°)**
1	N(1)–H(1)···O(7)[a]	0.876(18)	2.374(18)	3.0665(15)	136.1(15)
2	N(1)–H(1)···O(1W)[a]	0.84(2)	2.33(2)	3.0762(19)	148.3(17)
	O(1W)–H(1W)···O(7)	0.79(3)	2.11(3)	2.8664(17)	161(3)
	O(1W)–H(2W)···O(1L)	0.83(2)	1.97(2)	2.797(2)	171(2)

D, donor; H, hydrogen; A, acceptor. Symmetry transformation [a] = 1-x,1-y,1-z.

Table 5: Geometric features (distances, Å and angles,°) of the π···π stacking interactions in complexes **1** and **2**.

Complex	Cg(Ring I)···Cg(Ring J)	Cg···Cg(Å)	α (°)	Cg(I)···Perp(Å)	Cg(J)···Perp(Å)
1	Cg(4)···Cg(5)[c]	3.9495(8)	5.41(7)	3.7118(6)	3.6043(6)
	Cg(5)···Cg(5)[c]	3.8972(9)	0	3.6342(6)	3.6341(6)

Symmetry transformations: [c] = 2-x,1-y,2-z.

α = Dihedral angle between ring I and ring J. Cg(I)···Perp = Perpendicular distance of Cg(I) on ring J. Cg(J)···Perp = Perpendicular distance of Cg(J) on ring I. Cg(4) = Centre of gravity of the ring [C(6)-C(7)-C(8)-C(9)-C(10)-C(15)]; Cg(5) = Centre of gravity of the ring [C(10)-C(11)-C(12)-C(13)-C(14)-C(15)].

*$[Cu_2(L)_2(\mu_{1,3}\text{-}NCS)_2]\cdot DMF\cdot H_2O$ (**2**)*

Single crystal X-ray crystallography reveals that complex **2** is also a centrosymmetric dimer and it crystallizes in the triclinic space group $P2_1/n$. The asymmetric unit contains a square pyramidal copper(II) centre bonded to three donor atoms (N,N,O) of the deprotonated tridentate Schiff base (L^-) and end-on bridging anionic ligand cyanate leading to elongated (4+1) square pyramidal geometry. The perspective view of complex **2** with selective atom numbering scheme is depicted in Fig. 4. The Addison parameter value [τ= 0.167] indicates that the coordination sphere of copper(II) centre is close to the ideal square-pyramidal geometry. As usual for square pyramidal structures, copper(II) centres are slightly pulled out of the mean square planes towards the apical donor atoms at distance of -0.1349(2) Å in **2**. The three donor atoms of the Schiff base occupy the equatorial plane while each of the anionic ligand in the dimer occupies an equatorial position in one copper coordination sphere and an axial position at a longer distance in the other.

The $Cu–N_{imine}$ distance is significantly shorter 1.922(3) Å than the $Cu–N_{amine}$ distance 2.036(4) Å for **2**, as observed in similar complexes.[14] The copper(II)-nitrogen(anion) bond lengths in the equatorial plane range from 1.937(4)-1.979(5)Å, while the copper(II)-nitrogen(anion) axial bond lengths range from 2.442(5)-2.692(4) Å. The five membered chelate ring Cu(1)–N(1)–C(2)–C(3)–N(4) assumes intermediate conformation between half-chair and envelope being twisted on N(1)-C(2) with puckering parameters q(2) = 0.4307(16) Å and ϕ(2) = 263.97(16)°. Deviations of the coordinating atoms, N(1), N(4), O(7) and N(1'), from the least-square basal planes are 0.1165(14), -0.0556(12), 0.1221(11), and -0.0481(14) Å. The bridging Cu_2N_2 network is planar. The bridging pseudo-halides are quasi-linear with the N–C–S angle being 179.3(1)°. The intra dimer Cu···Cu distance is 5.6382(4) Å. Selected bond lengths and angles are given in Tables 2 and 3, respectively.

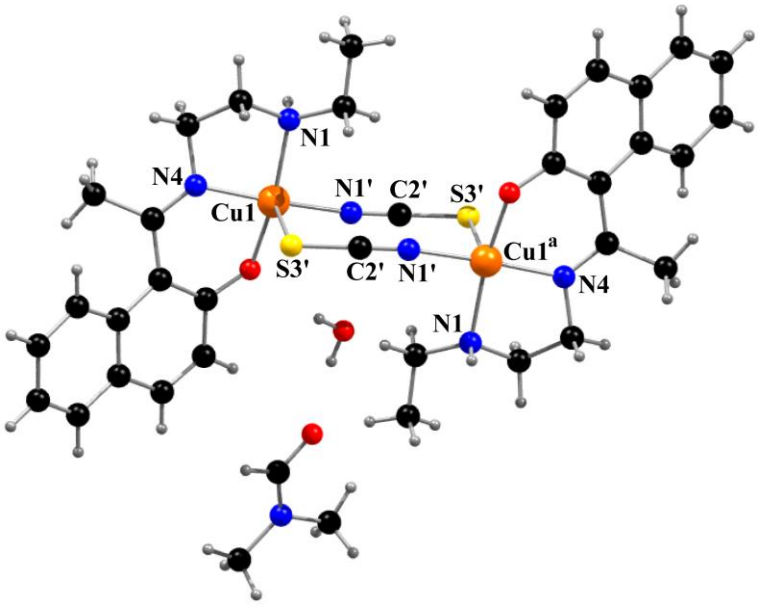

Fig. 4: Perspective view of complex **2** with selective atom numbering scheme. Hydrogen atoms have been omitted for clarity except solvent molecules. Symmetry transformation: [a] = 1-x,-y,1-z.

The hydrogen atoms H(1W) and H(2W), attached to the oxygen atom O(1W), are involved in hydrogen bonding interactions with the symmetry related the symmetry related phenoxo oxygen atom, O(7)[a] and oxygen atom, O(1L)[a] ([a] = 1-x,1-y,1-z), respectively. The hydrogen atom H(1), attached to nitrogen atom N(1), is engaged in bifurcated hydrogen bonding interactions with the symmetry related oxygen atoms O(1W)[a] and phenoxo oxygen atom, O(7)[a], ([a] = 1-x,1-y,1-z) leading to the formation of a chain (Fig. 5). The geometric features of C–H···π interactions are given in Table 6.

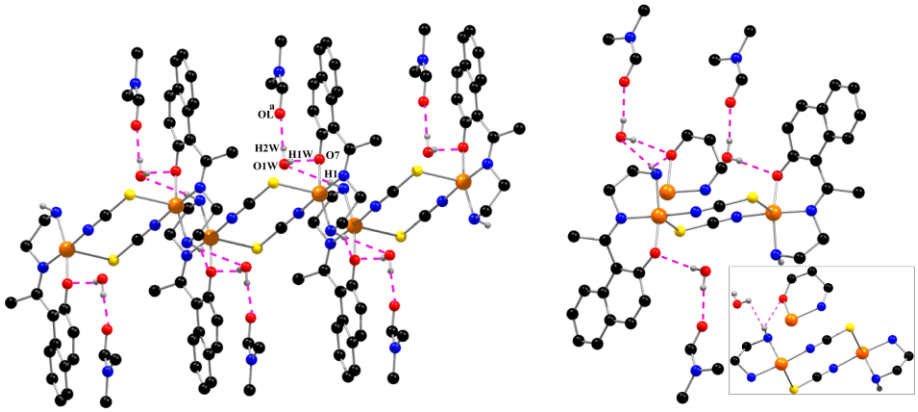

(a) **(b)**

Fig. 5: (a) One-dimensional hydrogen bonded chain structure of complex **2**. (b) Highlighted H-bonding interactions. Selected hydrogen atoms and ethyl group have been omitted for clarity. Symmetry transformation, [a] = 1-x, -y, 1-z.

Table 6: Geometric features (distances in Å and angles in °) of the C-H···π interactions obtained for complexes **1** and **2**.

Complex	C-H···Cg(Ring)	H···Cg	C-H···Cg (°)	C···Cg (Å)
1	C(16)–H(16C)···Cg(5)[d]	2.96	162	3.9081(16)
	C(3L)–H(3LA)···Cg(4)[e]	2.81	144	3.651(2)

2	C(3L)–H(3LB)···Cg(4)[f]	2.74	149	3.618(2)
	C(4L)–H(4LA)···Cg(3)[e]	2.73	141	3.544(2)
	C(4L)–H(4LC)···Cg(3)[f]	2.89	131	3.615(2)

Symmetry transformations: [d]= x,1/2-y,-1/2+z; [e]= 3/2-x,1/2+y,1/2-z; [f]= 3/2-x,-1/2+y,1/2-z

For complex **1**: Cg(5) = Centre of gravity of the ring [C(10)-C(11)-C(12)-C(13)-C(14)-C(15)];

For complex **2**: Cg(4) = Centre of gravity of the ring [C(10)-C(11)-C(12)-C(13)-C(14)-C(15)];

Cg(3) = Centre of gravity of the ring [C(6)-C(7)-C(8)-C(9)-C(10)-C(15)].

IR and electronic spectra

In the IR spectra of complexes **1** and **2**, strong and sharp bands around 1610 cm^{-1} were routinely noticed due to azomethine (C=N) groups of Schiff bases.[16] One moderately strong band in the region of 3200-3228 cm^{-1} in the IR spectrum of both complexes may be assigned to N–H stretching vibration.[17] The bands in the range of 2985-2860 cm^{-1} may be assigned to as alkyl C-H bond stretching vibrations.[18] One sharp and strong band at 2209 cm^{-1} in the IR spectrum of **1** indicates the presence of the N bonded cyanate group.[19] The μ-1,3 bridging mode of the thiocyanate group in complex **2** is confirmed by the splitting of the absorption band corresponding to the $\gamma_{C=N}$ asymmetric stretching at 2103 and 2053 cm^{-1} indicates the S- and N-coordination modes of the thiocyanate ligand respectively.[20,21] Two medium bands at 831 and 762 cm^{-1} may be attributed to ν(CS).[21]

The broad absorption bands around 595 nm were observed for both complexes i.e. in the visible region due to d-d transitions. The absorption bands around 310 nm may be assigned to

intraligand $\pi^* \leftarrow$ n transitions of azomethine (C=N) function of Schiff base. [22] The band around 390 nm may be attributed to LMCT transition.[23]

Magnetic properties

Variable temperature (2–300 K) magnetic susceptibility data were collected for microcrystalline samples of both complexes. The agreement factor R is defined as $R = \Sigma_i[(\chi_M T)_{obsd} - (\chi_M T)_{calcd}]^2 / \Sigma_i[(\chi_M T)_{obsd}]^2$. The temperature independent paramagnetism (TIP) was taken as -338×10^{-6} and -369×10^{-6} $cm^3 K\ mol^{-1}$ for complexes **1** and **2**, respectively.

Since both complexes consist of isolated copper(II) dimers with double pseudo-halide bridges, a simple Bleaney-Bowers dimer model for two $S = {}^1/_2$ ions was used to fit the magnetic data. This model reproduces very satisfactorily magnetic properties in the whole temperature range. Therefore, the magnetic behaviour ($\chi_M T$ vs T and χ_M vs T plots) was simulated using the standard Heisenberg-Dirac-van Vleck Hamiltonian, $\hat{H} = -2JS_1 \cdot S_2 + \mu_B gSH$, where all the parameters have their usual meanings.

Complex 1

A $\chi_M T$ versus T plot (χ_M is the molar susceptibility for two copper(II) ions) for complex **1** is shown in Fig. 6. The value of χ_M T for **1** at 300 K is 0.834 cm^3 K mol^{-1}, which is as expected for two magnetically quasi-isolated spin doublets ($g > 2.00$). The $\chi_M T$ values remains practically constant from 25–300 K. Below 25 K, there is an abrupt increase of $\chi_M T$, reaching a value of 1.034 cm^3 K mol^{-1} at 2 K. The χ_M values increase monotonically when the temperature decreases (Fig. 6). The fit of the experimental data yields the following values: $g = 2.115(2)$; $J = 0.97(6)$ cm^{-1}; $R = 5.4 \times 10^{-3}$.

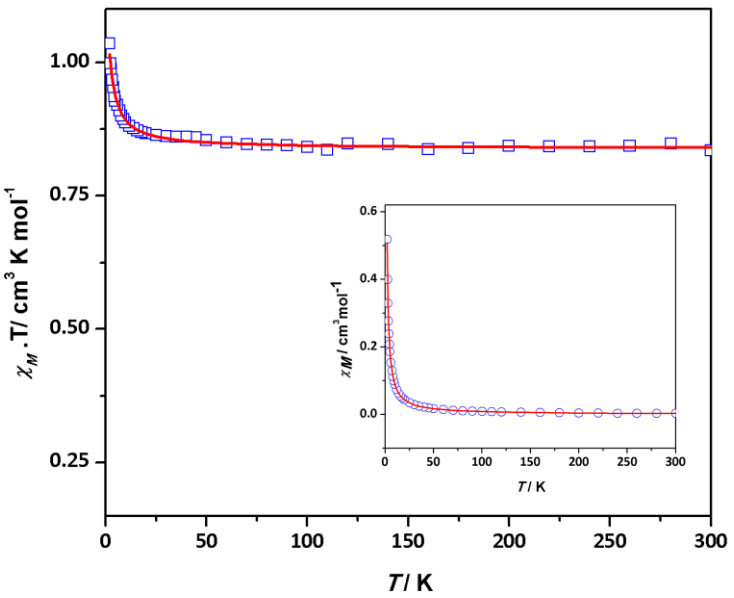

Fig. 6: Plot of $\chi_M T$ vs T for a powder sample of complex **1** in a 1 T external magnetic field. Experimental data are shown as blue squares and the best fit is represented by the red line. Inset shows plot of χ_M vs T where the experimental data are shown as blue circles and the best fit is represented by the red line.

Complex 2

The $\chi_M T$ and χ_M (inset) versus T plots (χ_M is the molar magnetic susceptibility for two copper(II) ions) are shown in Fig. 7. The value of $\chi_M T$ at 300 K is 0.822 cm^3 K mol^{-1}, which is as expected for two magnetically quasi-isolated spin doublets ($g > 2.00$). The $\chi_M T$ values remain practically constant until around 30 K, then decreases slowly and finally drops to 0.697 cm^3 K mol^{-1} at 2 K due to antiferromagnetic exchange coupling between copper(II) centres. No maximum was found in the χ_M versus T plot. The global feature is characteristic of weak antiferromagnetic coupling. The best fit was achieved for g = 2.09(1) and J = - 0.6(1) cm^{-1} (R= 2.9 × 10^{-2}). The relatively high value of R originates probably from the strong intermolecular H-bonding interactions in **2.**

Fig. 7: Plot of $\chi_M T$ vs T for a powder sample of complex **2** in a 1 T external magnetic field. Experimental data are shown as blue squares and the best fit is represented by the red line. Inset shows plot of χ_M vs T where the experimental data are shown as blue circles and the best fit is represented by the red line.

Magneto-structural correlation

Complex **1** is a double end-on cyanate bridged dinuclear copper(II) complex with a tridentate N_2O donor Schiff base. Although Cu–N–Cu angle is the key factor in determining the sign of J value, when pseudo-halide ligand bridges two copper(II) centres in end-on, basal–basal manner,[24] there is no meaningful correlation between Cu–N–Cu angle and *J* value in in basal–apical pseudo-halide bridged dinuclear copper(II) complexes.[25] This is because the single unpaired electron of copper(II) resides in $dx^2–y^2$ orbital, which lies essentially in the basal plane (XY plane) of the copper(II) centre having square pyramidal geometry; and therefore the magnetic orbital has only a small contribution in the direction of Z-axis (i.e. in the direction of second copper(II) linked via pseudo-halide bridge). Thus there is practically no overlap between the magnetic orbitals. Therefore the weak interactions amongst the copper(II) centres in end-on basal–apical cyanate bridged dinuclear complex **1** may be linked with the square pyramidal geometry of copper(II) centre. Table 7 gathers all end-on cyanate bridged and a few pseudo-halide bridged dinuclear copper(II) complexes along with τ values of copper(II) centres. Lower value of τ indicate less deviation from ideal square pyramidal geometry, and may be expected to have lower value of *J*.[5] However, this simple theory does not seem to be appropriate, as is evident from the data listed in Table 7.

Table 7: Main structural and magnetic parameters for end-on bridged copper(II) complexes with tridentate N_2O donor Schiff bases

Complex	Cu–Cu (Å)	Cu–N (basal) (Å)	Cu–N (apical) (Å)	Cu–N–Cu (0)	τ	*J* (cm^{-1})
LEKDIR[5a]	3.2715(8)	1.937(4)	2.692(4)	88.4(1)	0.001	0.513
GOYPUH[5b]	3.1558(5)	1.951(2)	2.528(2)	88.60(8)	0.049	-0.54
YADGUG[8b]	3.104(2)	1.999(1)	2.443(9)	88.3(4)	0.135	-2.63
IRIREG[10a]	3.1807(8)	1.998(3)	2.505(3)	89.2(1)	0.176	-8.5(5)
VOWJEY[3b]	3.199(7)	2.017(3)	2.490(3)	89.8(1)	0.273	1.07
NIKHUM[3c]	3.208(4)	1.984(18)	2.489(19)	87.7(7)	0.149	-10.16
NIKHOG[3c]	3.227(2)	2.005(5)	2.500(5)	90.8(2)	0.248	-4.18
NIKLAW[3c]	3.159(2)	1.983(5)	2.551(6)	84.3(2)	0.078	-1.43
JOPFIF[1a]	3.370(1)	1.968(2)	2.404(2)	100.4(8)	0.341	-11.4
GOYPIV[5b]	3.158(2)	2.009(2)	2.483(2)	88.68(6)	0.172	-2.28
LEKDEN[5a]	3.287(9)	1.979(5)	2.442(5)	95.5(2)	0.065	-2.313
Complex 1	3.2354(4)	1.938(1)	2.722(1)	86.23(4)	0.102	0.97(6)

On the other hand, complex **2** features an end-to-end thiocyanate bridged dimer. The weak antiferromagnetic coupling (J = - 0.6(1) cm^{-1}) is obviously due to the longer distance (5.6382(4) Å) among copper(II) centres. Only one similar dinuclear copper(II) complex with

Schiff base blocking ligand bridged by end-to-end thiocyanate is reported in literature (Table 8).[12b]

Table 8: Main structural and magnetic parameters for end-to-end bridged copper(II) complexes with tridentate N_2O donor Schiff bases

Complex	**Cu–Cu** (Å)	***J*** **(cm^{-1})**
MAQRAY[12b]	5.8629(6)	-1.71(1)
Complex **2**	5.6382(4)	-0.6(1)

Conclusion

The whole work can be concluded in two statements. Firstly, the use of different pseudo-halides with different bridging ability (i.e. cyanate and thiocyanate) can regulate the electronic and steric demands which could effectively modulate the structural versatility of complexes: cyanate with least bridging ability forms end-on bridged dimer, whereas thiocyanate with moderate bridging ability forms end-to-end bridgrd dimer. Secondly, comparison of the structures and the results of magnetic properties with previously related reported dinuclear copper(II) complexes with tridentate N_2O donor Schiff bases reveals that the magnetic exchange in such systems is governed by combined effects of several parameters. Synthesis and characterization of more complexes may be needed to arrive at any concrete generalization.

Notes and references

Electronic supplementary information (ESI): Experimental details, X-ray crystallographic data and Instrumentation details, Hirshfeld surfaces. CCDC 1580147 and 1580148 contain the supplementary crystallographic data for complexes **1** and **2**, respectively. These data can be obtained free of charge via http://www.ccdc.cam.ac.uk/conts/retrieving.html, or from the Cambridge Crystallographic Data Centre, 12 Union Road, Cambridge CB2 1EZ, UK; fax: (+44) 1223-336-033; or e-mail: deposit@ccdc.cam.ac.uk.

1. (a) S. Jana, B. K. Shaw, P. Bhowmik, K. Harms, M. G. B. Drew, S. Chattopadhyay and S. K. Saha, *Inorg. Chem.* 2014, **53**, 8723−8734. (b) Y. Wang, Y. -X. Che and J. -M. Zheng, *Inorg. Chem. Commun.*, 2012, **21**, 69–71; (c) L. -Z. Chen, D. -D. Huang, J. -Z. Ge and F. -M. Wang, *Inorg. Chim. Acta*, 2013, **406**, 95–99; (d) R. Biswas, Y. Ida, M. L. Baker, S. Biswas, P. Kar, H. Nojiri, T. Ishida and A. Ghosh, *Chem. Eur. J.*, 2013, **19**, 3943–3953. (e) M. Das and S. Chattopadhyay, *Polyhedron*, 2013, **50**, 443–451.

2. (a) C. Biswas, S. Chattopadhyay, M. G. B. Drew and A. Ghosh, *Polyhedron*, 2007, **26**, 4411-4418; (b) H. Y. Zang, Y. Q. Lan, G. S. Yang, X. L. Wang, K. Z. Shao, G. J. Xu and Z. M. Su, *CrystEngComm.*, 2010, **12**, 434–445; (c) M. Das, S. Chatterjee and S. Chattopadhyay, *Polyhedron*, 2014, **68**, 205–211; (d) Z. N. Chen, H. X. Zhang, K. B. Yu, K. C. Zheng, H. Cai and B. S. Kang, *J. Chem. Soc., Dalton Trans.*, 1998, 1133–1136; (e) A. Bacchi, M. Carcelli, T. Chiodo and P. Pelagatti, *CrystEngComm.*, 2010, **12**, 4226–4230;

3. (a) S. Koner, S. Saha, T. Mallah and K.-I. Okamoto, *Inorg. Chem*., 2004, **43**, 840-842; (b) P. P. Chakrabarty, S. Giri, D. Schollmeyer, H. Sakiyama, M. Mikuriya, A. Sarkar and S. Saha, *Polyhedron*, 2015, **89**, 49-54; (c) S. Mondal, P. Chakraborty, N. Aliaga-Alcalde and S. Mohanta, *Polyhedron*, 2013, **63**, 96-102; (d) M. Zbiri, S. Saha, C. Adhikary, S. Chaudhuri, C. Daul and S.

Koner, *Inorg. Chim. Acta*, 2006, **359**, 1193-1199; (e) C. Adhikary, R. Sen, G. Bocelli, A. Cantoni, S. Chaudhuri and S. Koner, *J. Coord. Chem*., 2009, **62**, 3573-3582.

4 (a) C. Adhikary and S. Koner, *Coord. Chem. Rev.,* 2010, **254**, 2933-2958 and references there in.

5. (a) A. Bhattacharyya, A. Bauzá, S. Sproules, L. S. Natrajan, A. Frontera and S. Chattopadhyay, *Polyhedron* 2017, **137**, 332–346; (b) P. Bhowmik, A. Bhattacharyya, K. Harms, S. Sproules and S. Chattopadhyay, *Polyhedron*, 2015, **85**, 221-231.

6. (a) Zhong-Lu You, Lin Zhang, Da-Hua Shi, Xiao-Ling Wang, Xiao-Fang Li and Yu-Ping Ma, *Inorg.Chem.Commun.*, 2010, 13, 996-998; (b) A. Bhattacharyya, B. N. Ghosh, S. Herrero, K. Rissanen, R. Jiménez-Aparicio and S. Chattopadhyay, *Dalton Trans.*, 2015, **44**, 493-497; (c) S. Roy, A. Bhattacharyya, S. Herrero, R.Gonzalez-Prieto, A. Frontera, and S. Chattopadhyay, *ChemistrySelect* 2017, **2**, 6535–6543.

7. (a) S. Mukherjee and P. S. Mujherjee, *Acc. Chem. Res.*,2013, **46**, 2556-2566; (b) S. Mukherjee and P.S. Mujherjee, *Dalton Trans.*, 2013, **42**, 4019-4030; (c) P. Talukder, A. Datta, S. Mitra, G. Rosair, M. S. E. Fallah and J. Ribas, *Dalton Trans*., 2004, 4161-4167; (d) Rui-Hua Hui, Peng Zhou, Zhong-Lu You, *Synth React Inorg Met Org nano-Met. Chem,* 2009, 39, 495-495.

8. (a) S. Jana, P. Bhowmik, M. Das, P. P. Jana, K. Harms and S. Chattopadhyay, *Polyhedron*, 2012, **37**, 21–26; (b) M. S. Ray, A. Ghosh, S. Chaudhuri, M. G. B. Drew and J. Ribas, *Eur. J. Inorg. Chem.*, 2004, 3110-3117; (c) S. Paul, R. Clerac, N. G. R. Hearns and D. Ray, *Cryst. Growth Des*., 2009, **9**, 4032-4040;

9. S. Sikorav, I. Bkouche-Waksman and O. Kahn, *Inorg. Chem.* 1984, **23**, 490-495.

10. (a) S. Koner, S. Saha, T. Mallah and K.-I. Okamoto, *Inorg. Chem*., 2004, **43**, 840-842; (b) S. Mondal, P. Chakraborty, N. Aliaga-Alcalde and S. Mohanta, *Polyhedron*, 2013, **63**, 96-102; (c) P. P. Chakrabarty, S. Giri, D. Schollmeyer, H. Sakiyama, M. Mikuriya, A. Sarkar and S.Saha, *Polyhedron*, 2015, **89**, 49-54

11. a) Z. Shen, J. L. Zuo, Z. Yu, Y. Zhang, J. F. Bai, C. M. Che, H. K. Fun, J. J. Vittal and X. Z. You, *J. Chem. Soc., Dalton Trans.*, 1999, 3393-3398; (b) S. Dalai, P. S. Mukherjee, T. Mallah, M. G. B. Drew and N. R. Chaudhuri, *Inorg. Chem. Commun.,* 2002, **5**, 472-474; (c) Z. Shen, J. L. Zuo, S. Gao, Y. Song, C. M. Che, H. K. Fun and X. Z. You, *Angew. Chem., Int. Ed*., 2000, **39**, 3633-3635.

12. (a) Y. S. You, J. H. Yoon, H. C. Kim and C. S. Hong, *Chem. Commun*., 2005, 4116-4118; (b) S. Banerjee, M. G. B. Drew, C.-Z. Lu, J. Tercero, C. Diaz and A. Ghosh, *Eur. J. Inorg. Chem.,* 2005, 2376–2383.

13. S. Khan, A. A. Masum, M. M. Islam, M.G.B. Drew, A. Bauzá, A. Frontera and S. Chattopadhyay, *Polyhedron* 2017, **123**, 334-343.

14. P. K. Bhaumik, K. Harms and S. Chattopadhyay, *Polyhedron*, 2014, **67**, 181–190.

15. D. Cremer and J. A. Pople, *J. Am. Chem. Soc.*, 1975, **97**, 1354-1358.

16. S. Khan, S. Jana, M. G. B. Drew, A. Bauzá, A. Frontera and S.Chattopadhyay, *RSC Adv.* 2016, **6**, 61214–61220.

17. M. Das, S. Chatterjee, K. Harms, T. K. Mondal and Chattopadhyay, S. *Dalton Trans.* 2014, **43**, 2936–2947.

18. S. Roy, K. Harms, and S. Chattopadhyay, *Polyhedron* 2015, **91**, 10-17.

19. S. Thakurta, R. J. Butcher, C. J. Gomez-García, E. Garribba and S . Mitra, *Inorg. Chim. Acta* 2010, **363**, 3981−3986.

20. (a) P. C. H. Mitchell and R. J. P. Williams, *J. Chem. Soc.,* 1960, 1912-1918; (b) R. A. Bailey, S. L. Kozak, T.W. Michelsen and W.N. Mills, *Coord. Chem. Rev*., 1971, **6**, 407-445.

21. A. Sabatini and I. Bertini, *Inorg. Chem.* 1965, **4**, 959–961.

22. U. Singh, M. M. Dar, S. Anayutullah, H. Alam, N. Manzoor, S. Ahmed Al-Thabaiti and A. A. Hashmi, *J. Coord. Chem*., 2015, **68**, 2096-2106.

23. S. Roy, T. Basak, S. Khan, M. G. B. Drew, A. Bauzá, A. Frontera and S. Chattopadhyay, *ChemistrySelect* 2017, **2**, 9336–9343.

24. (a) S.S. Tandon, L.K. Thompson, M.E. Manuel and J.N. Bridson, *Inorg. Chem.* 1994, **33**, 5555-5570; (b) E. Ruiz, J. Cano, S. Alvarez and P. Alemany, *J. Am. Chem. Soc.* 1998, **120**, 11122-11129.

25. (a) P. Manikandar, R. Muthukumaran, K.R.J. Thomas, B. Varghese, C.V.R. Chandramouli and P.T. Manoharan, *Inorg. Chem.* 2001, **40**, 2378-2389; (b) X.J. Lin, Z. Shen, Y. Song, H.J. Xu, Y.Z. Li and X.Z. You, *Inorg. Chim. Acta* 2005, **358**, 1963-1969.

Electronic Supplementary Information

End-on cyanate or end-to-end thiocyanate bridged dinuclear copper(II) complexes with a tridentate Schiff base blocking ligand: Synthesis, structure and magnetic studies

Samim Khan,[a] Stephen Sproules,[b] Louise S. Natrajan,[c] Klaus Harms,[d] Shouvik Chattopadhyay[a,*]

[a] *Department of Chemistry, Inorganic Section, Jadavpur University, Kolkata – 700 032, India.*

[b]*WestCHEM, School of Chemistry, University of Glasgow, Glasgow G12 8QQ, United Kingdom.*

[c]*School of Chemistry, The University of Manchester, Oxford Road, Manchester M13 9PL, United Kingdom.*

[d]*Fachbereich Chemie, Philipps-Universität Marburg, Hans-Meerwein-Straße, D-35032 Marburg, Germany.*

Experimental Section

All chemicals were of reagent grade and used as purchased from Sigma-Aldrich without further purification.

Physical Measurements

Elemental analysis (carbon, hydrogen, and nitrogen) was carried out using a Perkin-Elmer 2400 II elemental analyzer. IR spectra in KBr (4000-500 cm^{-1}) were recorded using a Parkin Elmer RXI FTIR spectrophotometer. Electronic spectra in acetonitrile (1000–200 nm) were recorded in a Hitachi U-3501 spectrophotometer. The XRD data of the powdered sample

were collected on a Bruker D8 Advance X-ray diffractometer using with Cu K_α radiation (λ= 1.548 Å) generated at 40 kV and 40 mA. The PXRD spectra were recorded in a 2θ range of 5–50° using 1-D Lynxeye detector at ambient conditions. Electro-spray ionization mass spectra were recorded with Waters QTOF Micro YA263. A Quantum Design MPMSXL SQUID (Superconducting Quantum Interference Device) magnetometer was used to measure the variable-temperature magnetic properties. The temperature range was 2–300 K under an applied magnetic field of 5000 Oe. The signal of the sample holder was taken into account to correct the measured data, as well as the molar diamagnetic corrections for the compound, which were calculated on the basis of Pascal's constants.[1-2] Fits were performed using the program *julX*.

X-ray crystallography

Single crystals of both complexes were used for data collection using a Bruker D8 QUEST area detector diffractometer equipped with graphite-monochromated Mo K_α radiation (λ = 0.71073 Å) at 100 K. The molecular structures were solved by direct method and refined by full-matrix least squares on F^2 using SHELXL-2016.[3] X-ray intensity data were measured. The frames were integrated with the Bruker SAINT Software package using a wide-frame algorithm. Non hydrogen atoms were refined anisotropically. Hydrogen atoms attached to oxygen and nitrogen atoms were located by difference Fourier maps and were kept at fixed positions. Other hydrogen atoms were placed in their geometrically idealised positions and constrained to ride on their parent atoms. Numerical and/or multi-scan absorption corrections were applied to the data using the program SADABS.[4]

Hirshfeld surfaces

Hirshfeld surface analysis was explored to evaluate the structural flexibility and magnitude of each interchain interaction in both complexes. Hirshfeld surfaces[5-7] and associated 2D-fingerprint[8-10] plots were obtained using Crystal Explorer 3.[11] This analysis is useful for the evaluation of closest intermolecular atomic contacts, even in complex crystal structures.[12]

X-ray powder diffraction pattern

The experimental powder x-ray diffraction patterns of the bulk products agree well with the simulated XRD patterns generated from cif. This indicates purity of the bulk samples. Fig. S1 and Fig. S2 show the experimental and simulated XRD patterns for complexes **1** and **2,** respectively.

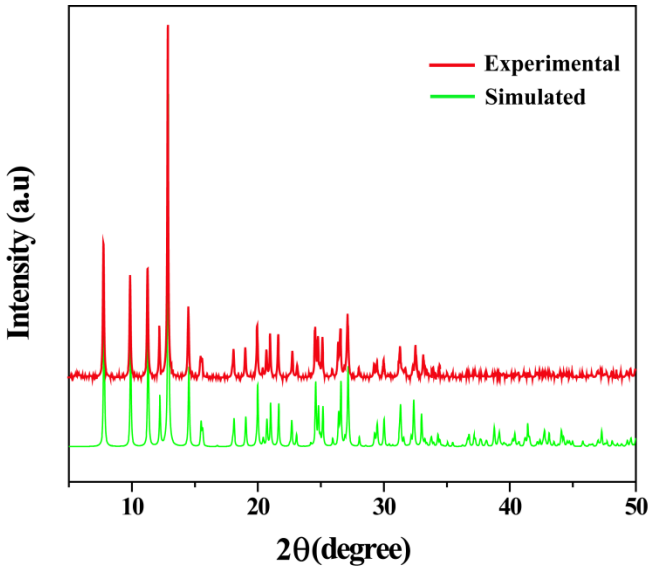

Fig. S1: Experimental and simulated powder XRD patterns of the complex **1** confirming the purity of bulk material.

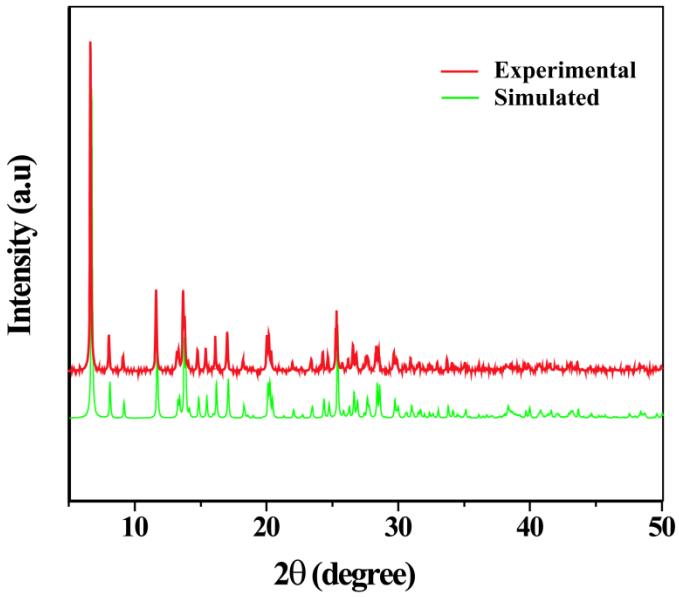

Fig. S2: Experimental and simulated powder XRD patterns of the complex **2** confirming the purity of bulk material.

Hirshfeld surface analysis

The Hirshfeld surfaces of both complexes, mapped over d_{norm}, shape index and curvedness, are illustrated in Fig. S3. The intermolecular interactions appear as distinct spikes in the 2D fingerprint plot (Fig. S4). we can decompose the fingerprint plot to highlight separate interactions.[13] The common features of Hirshfeld surfaces is the widespread presence of several red spots that are mostly recognized as C···H, O···H and N···H contacts. The proportions of C···H/H···C, interactions comprise 21.3 and 15.9% of the total Hirshfeld surfaces, respectively for each molecule of for **1** and **2**, whereas O···H/H···O interaction comprises of 19.1 and 11.9% to the total Hirshfeld surfaces, respectively for **1** and **2**.

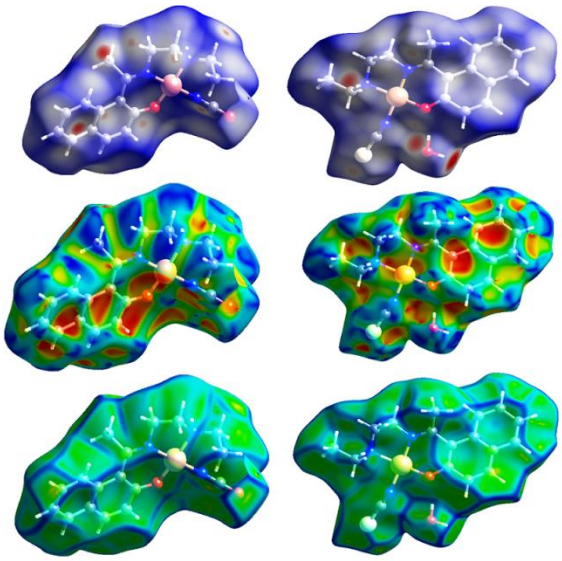

Fig. S3: Hirshfeld surfaces mapped with d_{norm} (top), shape index (middle), curvedness (bottom) for complexes **1** and **2**.

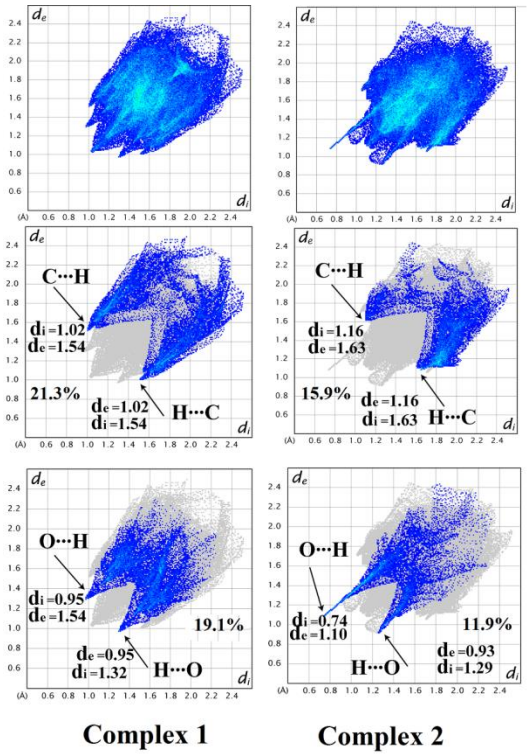

Fig. S4: 2D fingerprint plots: Full (top); O···H/H···O (middle) N···H/H···N (bottom) interactions contributed to the total Hirshfeld surface area of complexes **1** and **2**.

References

1. P. Pascal, *Ann. Phys. Chim.* 1910, **19**, 5*; Ann. Phys. Chim.* 1912, **25**, 289*; Ann. Phys. Chim.* 1913, **28**, 218.

2. G. A. Bain, J. F. Berry, *J. Chem. Educ*. 2008, **85**, 532-536.

3. G. M. Sheldrick, *Acta crystallographica. Section C, Structural chemistry* 2015, **71**, 3–8.

4. SADABS. Bruker AXS area detector scaling and absorption correction, Bruker AXS Inc., Madison, Wisconsin, USA, **2014**.

5. M. A. Spackman and D. Jayatilaka, *CrystEngComm,* 2009, **11**, 19-32.

6. F. L. Hirshfeld, *Theor. Chim. Acta,* 1977, **44**, 129-138.

7. H. F. Clausen, M. S. Chevallier, M. A. Spackman and B. B. Iversen, *New J. Chem*., 2010, **34**, 193-199.

8. A. L. Rohl, M. Moret, W. Kaminsky, K. Claborn, J. J. McKinnon and B. Kahr, *Cryst. Growth Des*., 2008, **8**, 4517-4525.

9. A. Parkin, G. Barr, W. Dong, C. J. Gilmore, D. Jayatilaka, J. J. McKinnon, M. A. Spackman and C. C. Wilson, *CrystEngComm* 2007, **9**, 648-652.

10. M. A. Spackman and J. J. McKinnon, *CrystEngComm* 2002, **4**, 378-392.

11. S. K. Wolff, D. J. Grimwood, J. J. McKinnon, D. Jayatilaka and M. A. Spackman, Crystal Explorer 2.0; University of Western Australia: Perth, Australia, 2007. http://hirshfeldsurfacenet.blogspot.com/.

12. M. A. Spackman, and D. Jayatilaka, *CrystEngComm* 2009, **11**, 19−32.

13. M.A. Spackman and P.G. Byrom, *Chem. Phys. Lett.* 1997, **267**, 215–220.